

Construction of a 40-channel SQUID System and Its Application to Neuromagnetic Measurements

Y. H. Lee^{*a}, J. M. Kim^a, H. C. Kwon^a, Y. K. Park^a, J. C. Park^a,
D. H. Lee^b and C. B. Ahn^b

^a *Superconductivity Group, Korea Research Institute of Standards and Science*

^b *Department of Electrical Engineering, Kwangjuon University*

Received 3 July 2000

Abstract

A 40-channel superconducting quantum interference device (SQUID) system was constructed for measuring neuromagnetic fields. Main features of the system are the use of double relaxation oscillation SQUIDs (DROSs), and planar gradiometers measuring magnetic field components tangential to the head surface. The DROSs with high flux-to-voltage transfers enabled direct readout of the SQUID output by room-temperature dc preamplifiers and simple flux-locked loop circuits could be used for SQUID operation. The pickup coil is an integrated first-order planar gradiometer with a baseline of 40 mm. Average noise level of the 40 channels is around 1.2 fT/cm/ $\sqrt{\text{Hz}}$ at 100 Hz, corresponding to a field noise of 5 fT/ $\sqrt{\text{Hz}}$, operated inside a magnetically shielded room. The SQUID insert was designed to have low thermal load, minimizing the loss of liquid helium. The constructed system was applied to measure auditory-evoked neuromagnetic fields.

Keywords : SQUID, low-field measurement, biomagnetism

I. Introduction

As low-noise magnetic field sensors, superconducting quantum interference devices (SQUIDs) are widely used for the measurements of weak magnetic signals. One of the main application area of the SQUID is biomagnetism, in which magnetic fields from the parts of the human body (brain or heart, etc) are measured. Of these, neuromagnetic measurements, with a high spatial and temporal resolution, provide useful information on the function of the brain, and now neuromagnetism is becoming a new diagnostic tool [1], [2].

To localize sources of the magnetic field in the brain, we first measure the field distribution over the head and secondly solve the inverse problem. To

speed up the measurement and to eliminate the fatigue or habituation of the subject, we need a multichannel system with as many number of sensing channels as possible. As the number of channel increases, the compactness and the reliability of the SQUID sensor and its readout electronics become an important figure of merit.

To simplify the readout electronics, the flux-to-voltage transfer of the SQUID should be large enough such that direct readout of the SQUID output voltage by room-temperature preamplifier should be possible. Compared with the standard dc SQUIDs, the double relaxation oscillation SQUID (DROS) provides very large flux-to-voltage transfer and large modulation voltage, and thus simple flux-locked loop electronics can be used for SQUID operation [3], [4].

To realize a reliable sensor structure and also to simplify the construction of the pickup coil, a planar gradiometer where the thin-film pickup coil is

*Corresponding author. Fax: +82 42 868 5290
e-mail: yhlee@kriss.re.kr

integrated on the same substrate as the SQUID is desirable.

In this paper, we describe a compact low-noise 40-channel SQUID system for neuromagnetic measurements by combining two approaches : an integrated planar pickup coil and a DROS with large flux-to-voltage transfer. The fabrication and operation characteristics of the system were described.

II. Design of DROS planar gradiometer sensor

The DROS consists of a hysteretic dc SQUID (the signal SQUID) and a hysteretic junction (the reference junction), shunted by a relaxation circuit of an inductor and a resistor. Instead of the reference SQUID, we used the reference junction to remove the possibility of flux trapping by the reference SQUID and to eliminate the lines needed for the adjustment of a reference flux [5].

The schematic circuit drawing of the DROS planar gradiometer and the close-up view of the DROS are shown in Fig. 1(a) and (b), respectively. In an adequate bias current range, DROS functions as a comparator of the two critical currents ; the signal critical current and the reference critical current. Thus, the voltage output of the DROS behaves like a square-wave function as the signal flux changes, resulting in a very large flux-to-voltage transfer coefficient when the two critical currents are equal.

The signal SQUID is a Ketchen-type dc SQUID with two $100 \mu\text{m} \times 100 \mu\text{m}$ square holes connected in parallel. Including the slit inductance, the inductance of the signal SQUID is estimated to be 113 pH. The size of each Josephson junction in the signal SQUID is $4 \mu\text{m} \times 4 \mu\text{m}$, while the reference junction has a size of $5 \mu\text{m} \times 5 \mu\text{m}$. In terms of the area ratio, the reference critical current corresponds to 78 % of the maximum value of the signal critical current.

Since the intrinsic noise of the DROS is inversely proportional to the square root of the relaxation frequency, the relaxation frequency is designed to be as high as about 1 GHz. To achieve a stable and low-noise SQUID operation, we made a special emphasis on the damping of various resonances induced by inductances and capacitances [6].

The input coil consists of two series-connected

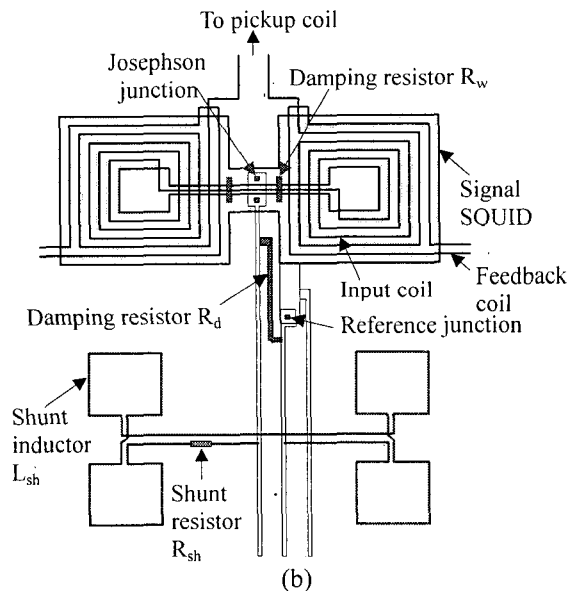
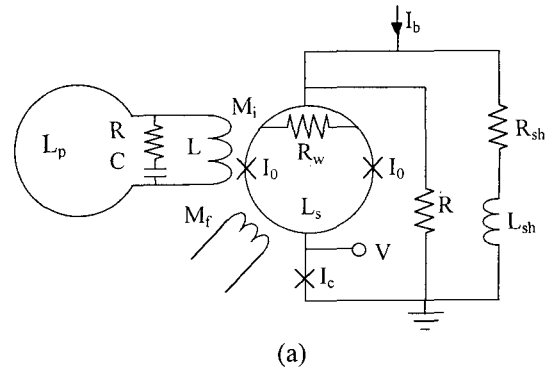


Fig. 1. (a) Schematic circuit drawing of the SQUID sensor and (b) close-up view of the DROS. Here I_b is the bias current, $2I_0$ is the critical current the signal SQUID and L_s is the inductance of the signal SQUID. R_{sh} and L_{sh} are the resistance and inductance of the relaxation circuit, respectively. R_d and R_w are damping resistors. M_i and M_f are the mutual inductances between the SQUID and the input coil (L_i), and the feedback coil, respectively. R_x and C_x are used to damp the input coil resonance. Output voltage V is measured across the reference junction I_{c2} .

coils, 15-turns each with a linewidth of $5 \mu\text{m}$, integrated on each SQUID loop and the input coil inductance is calculated to be 87 nH. Assuming the coupling coefficient with the SQUID to be 0.9, the mutual inductance between the input coil and the SQUID is estimated to be 2.8 nH. To damp resonances in the input coil, resistor-capacitor

damping circuit was connected in parallel with the pickup coil.

The pickup coil is a first-order gradiometer with two square coils connected in series, each with an outer dimension of $12 \text{ mm} \times 12 \text{ mm}$. The linewidth of the pickup coil is 0.5 mm and the baseline is 40 mm . The field-to-flux transfer of the flux transformer circuit is $0.95 \text{ nT}/\Phi_0$.

The sensors were fabricated on 3-inch Si wafers by a simple 4-level process based on Nb/ AlO_x /Nb junction technology. The junctions were defined by reactive ion etching and the insulation between metal layers was made by SiO_2 film deposited by plasma-enhanced chemical vapor deposition. The resistor is a reliable thin film of Pd. The overall size of the sensor is $12 \text{ mm} \times 52 \text{ mm}$ and 4 sensors were fabricated on each wafer. The fabricated sensors were glued onto printed circuit board (PCB) holders which has a size of $16 \text{ mm} \times 75 \text{ mm}$, where wiring copper leads were printed. At the end of the PCB holder, a 6-pin socket was soldered and the holder can be quickly replaced from the epoxy block.

Characterization of the sensors were done inside a magnetically shielded room with two layers of Mu-metal and one layer of Al, which has shielding factors of about 60 dB at 1 Hz and 90 dB at 100 Hz [7]. The fabricated DROSs had reference critical currents of around $10 \text{ }\mu\text{A}$ and the maximum modulation voltages of around $110 \text{ }\mu\text{V}$, which is about 2 times larger than that of dc SQUIDs. The flux-voltage curves of DROSs showed almost a step function of the applied field as shown in Fig. 2. The

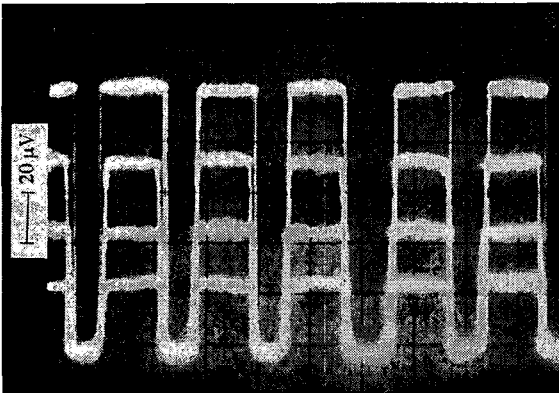


Fig. 2. Flux-voltage curves of a DROS at several bias currents. The maximum modulation voltage is larger than $100 \text{ }\mu\text{V}$.

maximum flux-to-voltage transfer is around $2 \text{ mV}/\Phi_0$, which is about 10 times larger than the transfer coefficient of standard dc SQUIDs. The flux noise is minimum when the reference critical current is around $10 \text{ }\mu\text{A}$. Among the sensors with reference critical currents of $5\text{--}20 \text{ }\mu\text{A}$, the average field noise value is about $5 \text{ fT}/\sqrt{\text{Hz}}$ at 100 Hz .

III. Readout electronics

The readout electronics of the SQUID consist of a preamplifier, main amplifier, integrator and SQUID controller. Because of the large transfer coefficient, the DROS output could be connected directly to a room-temperature dc preamplifier without an intermediate matching circuit. Fig. 3 shows the schematic circuit diagram of the flux-locked loop (FLL) electronics. The FLL circuits use a dc bias current and flux modulation is not used. The preamplifier is an instrumentation amplifier type made of LT1028 (Linear Technology) operational amplifiers and has an input voltage noise of $1.7 \text{ nV}/\sqrt{\text{Hz}}$ at 100 Hz and $5 \text{ nV}/\sqrt{\text{Hz}}$ at 1 Hz . With a typical transfer coefficient of $2 \text{ mV}/\Phi_0$, the preamplifier contributes an equivalent flux noise of $0.85 \text{ }\mu\Phi_0/\sqrt{\text{Hz}}$ at 100 Hz . In the frequency range $1\text{--}100 \text{ Hz}$, the preamplifier noise contribution is about 10 % of the total SQUID system noise [8].

Because of the large modulation voltage of DROSs, the FLL operation was quite stable against the offset voltage drift of the amplifier chain. The operation margin for the offset drift is about $15 \text{ }\mu\text{V}$ around the center of modulation voltage, this operation margin for the offset voltage is about 3 times larger than the dc SQUID with additional

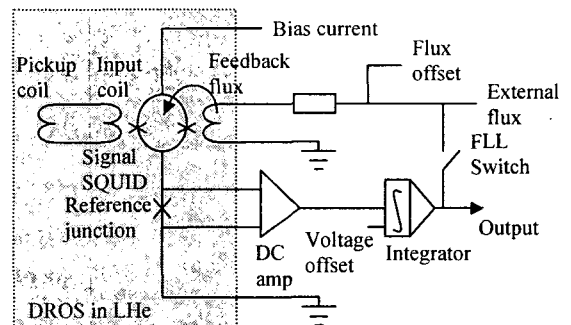


Fig. 3. Schematic diagram of the flux-locked loop circuit.

positive feedback [9].

The SQUID controller controls the bias current, integrator offset voltage and flux-lock point. The 40-channel system consists of 6 head boxes for FLL circuits and 3 sub-racks for SQUID controls. Each head box has 8 modular FLL circuits and were fixed on the ceiling of the shielded room. The control electronics are within an RF-shielded Al cabinet located outside the shielded room. The FLL outputs were passed through the 0.3-Hz high pass filters, 100-Hz low pass filters and 60-Hz notch filters, and amplified by gain-adjustable amplifiers. To remove high-frequency noises coming from the computer, 1-kHz low-pass filters were implemented between the controllers and the A/D card.

IV. 40-channel insert

The 40-channel insert consists of 16 rectangular epoxy rods, and each rod has 2~4 gradiometers in the x- and y-direction. The distance between two parallel gradiometers is 25 mm. The gradiometers were arranged to measure field components tangential to the body surface ; dB_x/dz and dB_y/dz , where z-axis is normal to the body surface. A tangential gradiometer sensitive to off-diagonal derivative has a magnetic field peak just above the current dipole when the detection coil is arranged perpendicular to the dipole direction. Thus, a less extensive sensor array is needed to get the essential field distribution [10].

In addition to the 40 channels, 4 reference channels, were added to pickup background noises and to apply adaptive filtering. Fig. 4 shows the assembled structure of the SQUID insert. To minimize thermal load, special care was taken in the choice of wire material and radiation shields. The low-thermal-conductivity manganin wires of 127 μm diameter were used for the bias current and the flux feedback. For the voltage lines, phosphorous bronze wires of 127 μm diameter were used. Since the resistance of the phosphorous bronze wire is about 9 Ω/m and the input current noise of LT1028 is 2 $\text{pA}/\sqrt{\text{Hz}}$ at 100 Hz, the voltage noise due to the wire resistance is about 18 $\text{pV}/\sqrt{\text{Hz}}$ at 100 Hz. This noise level is negligible compared with the input voltage noise of LT1028. All the wires were twisted in pair to eliminate magnetic coupling.

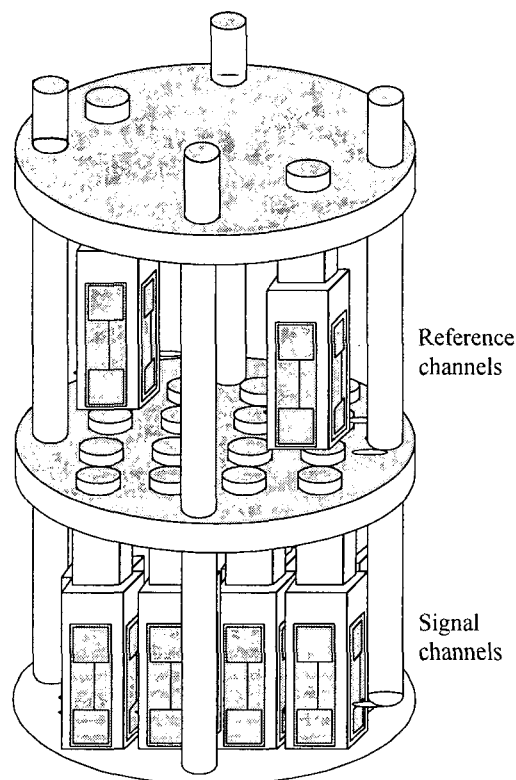


Fig. 4. Structure of the SQUID insert. 40 signal channel and 4 reference channels were used.

The connection between the SQUID assembly and the room-temperature were made of low-thermal-conductivity fiber-reinforced plastic tubes which has low thermal conductivity and high mechanical strength. The radiation baffles, made of multiple layers of Cu and styrofoam, were used to shield the heat coming from the dewar neck. The cold evaporating gas was used to cool the signal lines and the upper part of the insert. To compensate a dimensional change caused by thermal contraction of the insert on cooling, a sliding mechanism and spring were used which ensure the sensor end touches the dewar bottom all the time.

The liquid helium dewar has a flat tail with an inner tail diameter of 135 mm and the separation between 4.2 K and 300 K is 15 mm (Model FST-135-30, CTF Systems Inc.). The boil-off rate without any insert is 2.9 L/d. Because of the low thermal load, the boil-off rate of the complete 40-channel system could be as low as 3 L/d. The dewar has a liquid volume of 33 L and the refill period is 12 d.

V. Operation of 40-channel system

The 40-channel system consists of 40 SQUIDs, cryogenic insert, dewar, dewar gantry, FLL circuits, SQUID controllers, DC power supply, magnetically shielded room (MSR), RF-shielded cabinet, signal processing and source localization software.

Fig. 5(a) shows the magnetic field noise spectrum

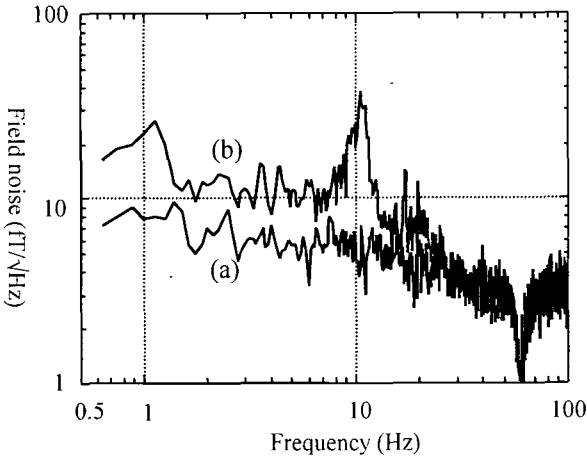


Fig. 5. (a) Noise spectrum of the DROS planar gradiometer measured inside a magnetically shielded room and (b) noise measured when the SQUID is placed over the occipital lobe of a normal subject with his eyes closed. Peaks at 1.2 Hz and 10 Hz are caused by heart beats and alpha rhythm, respectively.

of a gradiometer measured inside the MSR. Including all the noise contributions, like dewar thermal noise and the residual magnetic noise of the MSR, the SQUID system noise is $8 \mu\Phi_0/\sqrt{\text{Hz}}$ at 1 Hz and $4 \mu\Phi_0/\sqrt{\text{Hz}}$ at 100 Hz. Multiplied by the transfer coefficient of the flux transformer ($=0.25 \text{ fT/cm}/\Phi_0$), these correspond to the field gradient noises of $2 \text{ fT/cm}\sqrt{\text{Hz}}$ and $1 \text{ fT/cm}\sqrt{\text{Hz}}$, or field noises of $8 \text{ fT}/\sqrt{\text{Hz}}$ and $4 \text{ fT}/\sqrt{\text{Hz}}$ at 1 Hz and 100 Hz, respectively.

Fig. 5(b) shows the noise spectrum when the SQUID is placed over the occipital lobe of a subject, where the noise is the sum of system noise and the subject noise. The peak at 1.2 Hz is caused by heart beats and the peak at 10 Hz is the alpha rhythm from the visual cortex. From Fig. 5(a) and (b), we can see that SQUID system noise is about half of the brain noise in the frequency range of 1~10 Hz, meaning that the developed SQUID system can be applied to measure brain magnetic fields.

Among the 80 SQUIDs tested, the sensors have white (@ 100 Hz) noise values in the range of 4~7 $\text{fT}_{\text{rms}}/\sqrt{\text{Hz}}$, with an average of $5 \text{ fT}_{\text{rms}}/\sqrt{\text{Hz}}$. Assuming that the noise is flat in the frequency range of 1~100 Hz and have an average value of $7 \text{ fT}_{\text{rms}}/\sqrt{\text{Hz}}$, this corresponds to the noise amplitude of $70 \text{ fT}_{\text{rms}}$, or $100 \text{ fT}_{\text{peak}}$, in a measurement bandwidth of 100 Hz.

VI. Application to neuromagnetic measurements

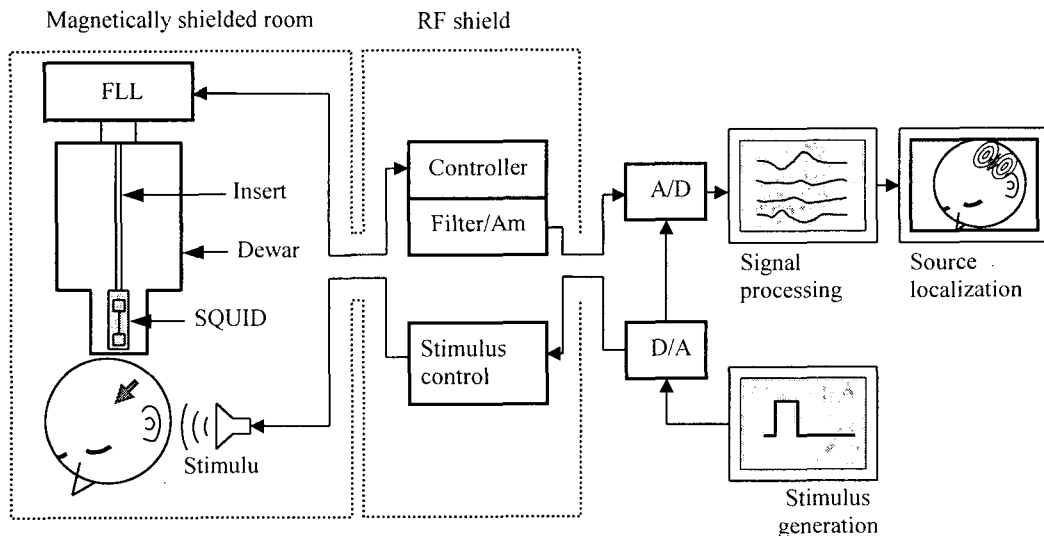


Fig. 6. Block diagram of the system for measuring auditory-evoked fields.

To demonstrate the usefulness of the developed system as a biomagnetic multichannel system, the 40-channel system was applied to measure neuromagnetic fields. Fig. 6 shows the schematic block diagram of the auditory-evoked fields measurement system. To apply non-magnetic auditory stimuli, a capacitive earphone was used with the signal lines twisted in pair. The software for the neuromagnetic measurements consists of DC offset removal, low-pass filter, 60-Hz elimination filter, spectrum analysis and field mapping.

Fig. 7 shows the x-component, 20-channel traces of auditory evoked responses. Auditory stimuli of a 1 kHz tone burst, 200 ms duration and 70 dB normal hearing level were applied to the left ear of a normal subject, and field measurements were done over the right temporal lobe. To remove the expectation effect, the inter-stimulus interval was varied randomly between 1~2 s. Sampling rate of the A/D card was 640/s. The traces were obtained after averaging of 128 times, using 0.3-Hz high pass filter, 100-Hz low pass filter and 60-Hz notch filter. Clear N100m peak, field component generated about 100 ms after the stimulus onset, was obtained. This peak corresponds to the response of the auditory primary cortex.

VII. Conclusion

We constructed a compact 40-channel SQUID system based on DROSSs and integrated planar

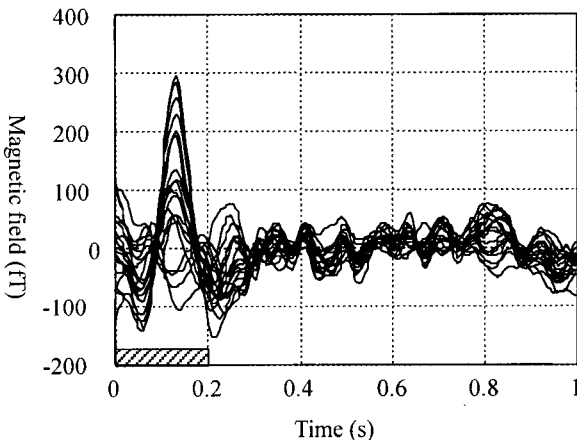


Fig. 7. Auditory-evoked field signals. 20 channels of the x-component are superposed. The hatched box on the time axis represents the stimulus duration (0~0.2 s).

gradiometers, and applied to measure neuromagnetic fields. The flux-to-voltage transfers of the DROSSs, more than 10 times larger than that of dc SQUIDs, were large enough to enable direct readout by room-temperature preamplifier, and simplified FLL circuits. And the large modulation voltage of DROSSs allowed stable FLL operation against the thermal drift of the amplifier offset voltage. Because of the low thermal load, the 40-channel insert itself had very low boil-off rate of less than 1 L/d. The average noise level of the SQUID system is about 5 fT/ $\sqrt{\text{Hz}}$ at 100 Hz, which is low enough for neuromagnetic measurements. By using the 40-channel system, neuromagnetic fields evoked by auditory stimuli were successfully measured.

Acknowledgments

This work was supported by the Ministry of Science and Technology, Republic of Korea.

References

- [1] M. Hämäläinen, R. Hari, R. J. Ilmoniemi, J. Knuutila and O. V. Lounasmaa, "Magnetoencephalography-theory, instrumentation, and applications to noninvasive studies of the working human brain," *Rev. Mod. Phys.* 65, 413-497 (1993).
- [2] J. P. Wikswo, Jr., "SQUID magnetometers for biomagnetism and nondestructive testing : Important questions and initial answers," *IEEE Trans. Appl. Supercond.*, 5, 74-120 (1995).
- [3] D. Drung, "Advanced SQUID readout electronics," in *SQUID Sensors: Fundamentals, Fabrication and Application*, ed. H. Weinstock, Dordrecht, Kluwer Academic Publishers, 63-116 (1996).
- [4] D. J. Adelerhof, H. Nijstad, F. Flokstra and H. Rogalla, "(Double) relaxation oscillation SQUIDs with high flux-to-voltage transfer: Simulations and experiments," *J. Appl. Phys.*, 76, 3875-3886 (1994).
- [5] Y. H. Lee, H. C. Kwon, J. M. Kim, Y. K. Park and J. C. Park, "Double relaxation oscillation SQUID with reference junction for biomagnetic multichannel applications," *Appl. Supercond.*, 5, 413-418 (1998).
- [6] Y. H. Lee, H. C. Kwon, J. M. Kim, Y. K. Park and J. C. Park, "Double relaxation oscillation SQUID with high flux-to-voltage transfer and its application to a biomagnetic multichannel system," *J. Kor. Phys. Soc.*, 32, 600-605 (1998).
- [7] Y. H. Lee, H. C. Kwon, J. M. Kim, C. M. Lim, S. K.

- Lee, Y. K. Park and J. C. Park, "Construction and characteristics of magnetically shielded room for biomagnetic measurements," *J. Kor. Magn. Soc.*, 6, 264-270 (1996).
- [8] Y. H. Lee, J. M. Kim, H. C. Kwon, S. K. Lee, C. M. Lim, Y. K. Park and J. C. Park, "Fabrication and noise characteristics of double relaxation oscillation superconducting quantum interference device with high flux-to-voltage transfer," *New Physics*, 39, 86-93 (1999).
- [9] T. Ryhanen, R. Cantor, D. Drung and H. Koch "Practical low-noise integrated dc superconducting quantum interference device magnetometer with additional positive feedback," *Appl. Phys. Lett.* 59, 228-230 (1991).
- [10] K. Tsukada, Y. Haruta, A. Adachi, H. Ogata, T. Komuro, T. Ito, Y. Tanaka, A. Kandori, Y. Noda, Y. Terada and T. Mitsui, "Multichannel SQUID system detecting tangential components of the cardiac magnetic field," *Rev. Sci. Instrum.*, 66, 5085-5091 (1995).